Local Density Inhomogeneities and Dynamics in Supercritical Water: A Molecular Dynamics Simulation Approach

Ioannis Skarmoutsos and Jannis Samios*

Department of Chemistry, Laboratory of Physical Chemistry, University of Athens, Panepistimiopolis 157-71, Athens, Greece

Received: February 14, 2006; In Final Form: August 7, 2006

Molecular dynamics atomistic simulations in the canonical ensemble (NVT-MD) have been used to investigate the "Local Density Inhomogeneities and their Dynamics" in pure supercritical water. The simulations were carried out along a near-critical isotherm ($T_r = T/T_c = 1.03$) and for a wide range of densities below and above the critical one ($0.2\ \rho_c - 2.0\ \rho_c$). The results obtained reveal the existence of significant local density augmentation effects, which are found to be sufficiently larger in comparison to those reported for nonassociated fluids. The time evolution of the local density distribution around each molecule was studied in terms of the appropriate time correlation functions $C_{\Delta_{\rho l}}(t)$. It is found that the shape of these functions changes significantly by increasing the density of the fluid. Finally, the local density reorganization times for the first and second coordination shell derived from these correlations exhibit a decreasing behavior by increasing the density of the system, signifying the density effect upon the dynamics of the local environment around each molecule.

1. Introduction

Following the literature, we can see that, in recent years, numerous experimental as well as theoretical investigations have been devoted to study the properties of supercritical fluids (SCFs). This interest is due to the fundamental question of their unique physicochemical properties and to their considerable practical importance.[1,2] It is well-known that the density of a SCF in the near critical region can be varied continuously from gaslike to liquidlike values even with a small change in pressure or temperature, causing corresponding changes in solute solvation and dynamics. This feature makes SCFs attractive alternatives to liquid solvents for several uses.[3]

The greatest variation of the solvent density is attained around the solvent's critical point, where the solvent compressibility, K_T, is very large. Note also that the compressibility, K_T, is directly related to the range over which microscopic fluctuations in density are correlated. As a result of this, the mean microscopic structure of a SCF near its critical point is that of an inhomogeneous medium with high and low-density regions. Generally, previous studies have led to the conclusion that undoubtedly density inhomogeneities are real and important phenomena in compressible SCFs. Moreover, experimental results have shown that density inhomogeneities in SCFs may be separate between the short-range (local density inhomogeneities-LDI) and long-range order ones. This consideration has been systematically discussed and eventually proposed in recent reviews,[4] wherein it is pointed out that the origins of these distinct density inhomogeneity effects are different.

To the best of our knowledge, only a few studies devoted to the short-range LDI in pure SCFs are reported up to now. On the other hand, studies on dilute SC solutions have shown that the local environment of a solute molecule may be in general different from that of a solvent one. In the case of attractive solutes immersed in SC solvents, several spectroscopic experiments suggest average local density that is 2−5 times greater than the bulk one.[5] Results on this field have been also reported from computer simulations (CS) used to model dilute solutions near the critical point [see ref 4 and references therein]. According to the recent literature, the local density augmentation in some nonpolar pure SCFs has been investigated by a number of authors using vibrational spectroscopy.[6−9] The results obtained indicated that also in that case, the average local density around a solvent molecule is greater than the system bulk density. Note, however, that the estimated magnitude of the local density augmentation is found to be sufficiently smaller compared to those obtained around a solute in dilute solutions.

From the theoretical point of view, there are only a handful CS studies devoted to the estimation of the local density augmentation of pure SCFs that have been reported up to now.[5,10−13] Song and Maroncelli[12] employed the MD simulation technique to investigate the local density augmentation in two pure SC fluids, namely one polar system (fluoroform) and a nonpolar one (ethane). The results obtained reveal that the local density augmentation in SC fluoroform is more pronounced than that in SC ethane. The authors in that study interpreted the behavior observed in terms of the strong electrostatic character of the intermolecular forces among the molecules in the polar fluid fluoroform.

It is well-known from the literature that supercritical water (SCW) is a highly reactive, polar and hydrogen-bonded solvent, which plays a crucial role in many chemical, biological, and industrial processes.[14] Despite that numerous experimental[15−21] and theoretical[22−32] investigations devoted to the study of several physicochemical properties of SCW and especially the hydrogen bonding network, have been published up to now, a thorough investigation of the static local density augmentation and corresponding dynamics in this fluid have never been reported in the literature so far. Therefore, in view of the great scientific and technological importance of SCW, a deeper and more quantitative understanding of the aforementioned effects be-

* Corresponding author fax: +30-210-7274752; e-mail: isamios@chem.uoa.gr.

10.1021/jp060955p CCC: $33.50
Published on Web 10/11/2006

comes indispensable in order to elucidate fundamental aspects of this particularly interesting molecular system.

The present work is a part of our theoretical investigations on the properties of supercritical solvents[33−38] and with this treatment we would like to provide useful quantitative information concerning the aforementioned properties of SCW. Concretely, the main goal of this work is to provide a comprehensive study of the bulk density dependence of the local density augmentation and local environment reorganization dynamics of SCW along selected state-points using the MD simulation technique. The quantitative knowledge of these effects in pure SCFs in general, is desirable toward a deeper understanding of the characteristic features related to the solvation effects in these solvents.

The paper is structured so that Section 2 describes the methodology employed to calculate the properties of interest, as well as the most important computational details. The results and discussion on the local intermolecular structure, local density augmentation and dynamics of the fluid are presented in Section 3. Finally, Section 4 contains the general conclusions and remarks drawn from the present study.

2. Methodology−Computational Details

In the following paragraphs, we will briefly describe the main quantities and relationships used to extract information concerning the LDI effects from the molecular trajectory generated during the simulation of the fluid. Note that the same methodology has been recently used in two similar studies of other model systems.[5,12]

We start with the average local density around a particle in the fluid defined in terms of the average number of particles (coordination number N_{co}) in the first and second solvation shell

$$N_{co}(\rho,R_c) = 4\pi\rho\int_0^{R_c} g_{com}(r)r^2dr \qquad (1)$$

In eq 1, $g_{com}(r)$ is the center of mass (COM) radial pair distribution function (pdf) and the quantity ρ denotes the bulk number density of the fluid at a given thermodynamic state point. R_c is a defined cutoff distance that specify the volume of the first or second solvation shell around a particle. As we can see in the following section, the R_c distance for the first shell has been estimated to be 4.22 Å, while as second solvation shell we have taken the region extending up to a distance of 6.75 Å from a molecule. Further to this, to estimate the excess local density in the near critical regime of a fluid, it is more convenient to calculate first of all the well-known *effective* local density, $\rho_{eff,l}$, according to the following relation

$$\rho_{eff,l}(\rho) = \frac{N_{co}(\rho)}{N_{co}(\rho_{ref})}\rho_{ref} \qquad (2)$$

The employed value of the reference density, ρ_{ref}, corresponds typically to a high liquidlike one, usually in the range $2-3\ \rho_c$. The cutoff distance, R_c, in eq 1 is determined as the position of the first minimum of the corresponding com pdf observed at this high reference density ρ_{ref}. This cutoff distance has been used to compute the *effective* local density, $\rho_{eff,l}$, of the first coordination shell in the simulations of the fluid at each bulk density of interest (state points: A−I).

To describe how far the average local density exceeds[5,12] the bulk one ρ, one uses the quantity of the excess local density (*augmentation*) defined as $\Delta\rho_{eff,l} = \rho_{eff,l} - \rho$, or alternatively the well-known *enhancement* factor $F_{enh} = (\rho_{eff,l}/\rho)$. Thus, in the framework of this simulation both quantities $\Delta\rho_{eff,l}$ and F_{enh} are computed as functions of the bulk density. The maximum value $\Delta\rho_{eff,l}$(max)obtained at a given bulk density provides a measure of the extent of the local density augmentation.

Additional insight into the problem of the short-range LDI in SCW is provided by the investigation of the time dependent distribution of the local density around each molecule. To the best of our knowledge, there is only one similar CS study in the literature devoted to the local density dynamics in a pure SC model fluid up to now. Concretely, in a two-dimensional CS study of a pure Lennard-Jones (LJ) monatomic model fluid, Tucker and co-workers[39b] investigated the time scale for the local solvent reorganization (local environment interconversion), which may control the dynamics of an arbitrary solvent molecule. In that work, the authors defined the instantaneous local-density deviation, $\Delta\rho_l(t)$, relative to the mean local one as $\Delta\rho_l(t) = \rho_l(t) - \langle\rho_l\rangle$, and calculated the dynamics of this quantity in terms of its autocorrelation function (acf), defined as follows[39a]

$$C_{\Delta_{\rho l}}(t) = \frac{\langle\Delta\rho_l(0)\cdot\Delta\rho_l(t)\rangle}{\langle[\Delta\rho_l(0)]^2\rangle} \qquad (3)$$

In the present treatment, the instantaneous local density $\rho_l(t)$ is calculated according to eq 2 applied at each time t; in other words, by computing the instantaneous coordination numbers within a cutoff distance R_c. At this point we need to emphasize that the property of interest is the correlation time, $\tau_{\Delta_{\rho l}}$, determined by the following integral relation

$$\tau_{\Delta_{\rho l}} = \int_0^\infty C_{\Delta_{\rho l}}(t)dt \qquad (4)$$

The correlation time $\tau_{\Delta_{\rho l}}$ corresponds to the local-density reorganization time. In other words, this is the time on which the local density around an arbitrary solvent varies significantly. It should be also emphasized here that the time $\tau_{\Delta_{\rho l}}$ calculated here is substantially different from the residence time or the so-called identity lifetime considered by other groups[39a,40a] in a few CS studies mainly of diluted mixtures. It is due to the fact that we investigate the lifetime for persistence of the local-number density fluctuation within a defined local region (shell) around a molecule, independent of the identity of the species that remain in the shell during a period.

The simulations of pure SCW were carried out in the canonical (NVT) statistical mechanical ensemble at $T = 666$ K, which for SCW ($T_c = 647.1$ K) corresponds to a reduced temperature $T_r = 1.03$ ($T_r = T/T_c$). We performed nine NVT-MD simulations for a series of densities in the range from 0.2 to 2.0 ρ_c. All the simulated thermodynamic state points are presented in Table 1. The intermolecular interactions are represented as pairwise additive with site−site LJ plus Coulomb interactions, due to the existence of the dipole moment of water molecules in their ground state.

Generally, the first task in this CS study has been to select an accurate potential model that is suitable in predicting the bulk, structural, and dynamic properties of the fluid at SC conditions. Following the literature, we can notice that a great number of models for water are often used in CS studies of this system mainly at liquid conditions. Among the most popular of them is the extended simple point charge (SPC/E)[41] potential model, which was chosen in the present treatment to simulate the interactions in SCW. Our choice is based upon previously reported CS results concerning the accuracy of this model in reproducing reasonably various properties of the fluid.[22,40] The SPC/E potential is a three-site fixed charge model, which

TABLE 1: Simulated Densities of SCW at $T/T_c = 1.03$[a]. The Coordination Numbers $N_{co}(\rho,R_c)$ Calculated up to a Cut-Off Distance R_c Corresponding to the Radius of the First and Second Coordination Shell at the Density $\rho = 2\rho_c$, Are Also Presented

thermodynamic state point		coordination number $N_c(\rho,R_c)$ [b]	
index	ρ/ρ_c[a]	first shell	second shell
A	0.1903	1.175	3.520
B	0.3529	1.971	6.441
C	0.6095	2.908	10.427
D	0.8597	3.623	13.767
E	1.1441	4.316	17.149
F	1.2660	4.609	18.612
G	1.4329	4.995	20.557
H	1.5654	5.325	22.174
I	2.0000	6.477	27.688

[a] For water, $\rho_c = 0.322$ g/cm^3, $T_c = 647.10$ K. [b] For the first shell, $R_c = 4.22$ Å, and for the second one, $R_c = 6.75$ Å.

provides vapor−liquid equilibrium properties that are in good agreement with experiment and with results obtained from other computationally too expensive models. In addition, this model has been successfully used in CS studies of water to elucidate the structure and dynamics of molecular clustering at vapor−liquid coexistence[42] and SC conditions.[25,26,28]

The MD simulations were carried out with 500 molecules in the simulation box using standard periodic boundary conditions while the minimum image convention was also employed for the calculation of the intermolecular forces. To make sure that the results obtained for the systems near the critical region are reliable, trial runs with larger system sizes have been also carried out. As a result, it is found that the estimated properties corresponding to systems of 864 molecules were converged to those of 500 ones. Note that in order to achieve equilibrium of the fluids at each thermodynamic state point of interest, the corresponding simulation was extended to at least 300 ps followed by at least 400 ps trajectory over which the structural and dynamic properties were calculated. In all simulations the time step was 1 fs. The equations of motion were integrated using a leapfrog-type Verlet algorithm and the Berendsen thermostat with a temperature relaxation of 0.5 fs was also used.[43] In addition, the intramolecular geometry of the species was constrained during the simulations by using the SHAKE method.[44,45] In each simulation, a cutoff radius of 1.2 nm was used to all LJ interactions and long-range corrections have been also taken into account. Moreover, the Ewald summation technique, with the use of the more exact approximation Newton−Gregory forward difference interpolation scheme,[45] was applied to account for the long-range electrostatic interactions.

3. Results and Discussion

As mentioned above, the appropriate quantity required to investigate the average local density of a fluid at a given thermodynamic state point is the corresponding com radial pdf, $g_{com}(r)$, of the system. It is, therefore, of particular interest to report briefly on the structural results obtained for SCW from our simulations.

In this NVT-MD study, we have calculated the radial pdfs between the atoms of different molecules as a function of density along a near-critical isotherm. However, we present here only the com pdfs of the simulated fluid, which, as it is known, are related to the properties associated with the LDI in the fluid. A thorough analysis of the structural results obtained from the site−site O−O and O−H pdfs is not a subject of investigation in this study and, for this reason, will be not presented hereinafter.

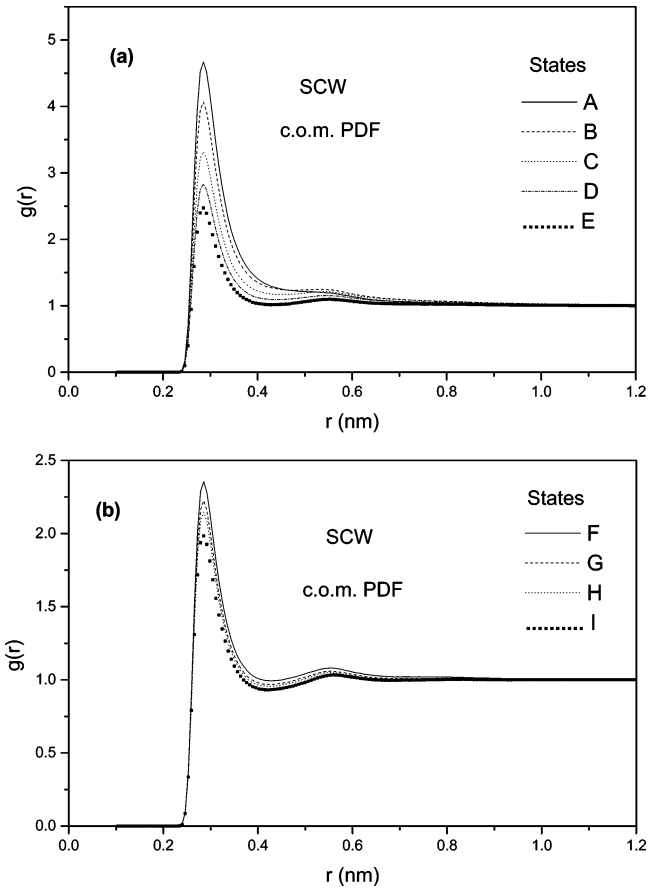

Figure 1. Calculated center of mass radial pair distribution functions of SCW at the thermodynamic state points A−E (a) and F−I (b).

The solvation intermolecular structure of SCW at the selected state points A−I is revealed from the simulated results shown in Figures 1 and 2. The com pdfs obtained are plotted in Figure 1a, b. From the comparison of these functions, it is seen that they exhibit a first peak localized at a distance of 2.85 Å, which remains almost invariant for all the simulated state points. In contrast to the first peak positions, we may also observe a density dependence of the first peak intensity at constant temperature as expected. Concretely, the amplitude of this peak decreases significantly from the value 4.67 (state A) to 1.98 (state I). In addition, the first peak is followed by a distinct minimum and further by a strongly reduced second maximum, while a third peak is not apparent in these functions. Note also that the value corresponding to the first minimum decreases on going from the lowest system density (state A) to the highest one (state I). It should be eventually mentioned here that the position of the first minimum of the com pdf at state point I ($\rho = 2\rho_c$) is observed at 4.22 Å and, according to the method employed to calculate local densities, this distance has been used as the cut off one in the calculation of the average local density of the first coordination shell at each state point under study (A−I).

As mentioned in the previous section, of most interest for the main purpose of this treatment is the behavior of the average coordination numbers, $N_{co}(\rho, R_c)$, obtained for the first coordination shell of a particle up to the cut off distance R_c as a function of the bulk system density ρ and at $T_r = 1.03$. Values of $N_{co}(\rho, R_c)$ are presented in Table 1. In addition, Figure 2a shows the values of $N_{co}(\rho, R_c)$ versus ρ/ρ_c along the isotherm $T_r = 1.03$.

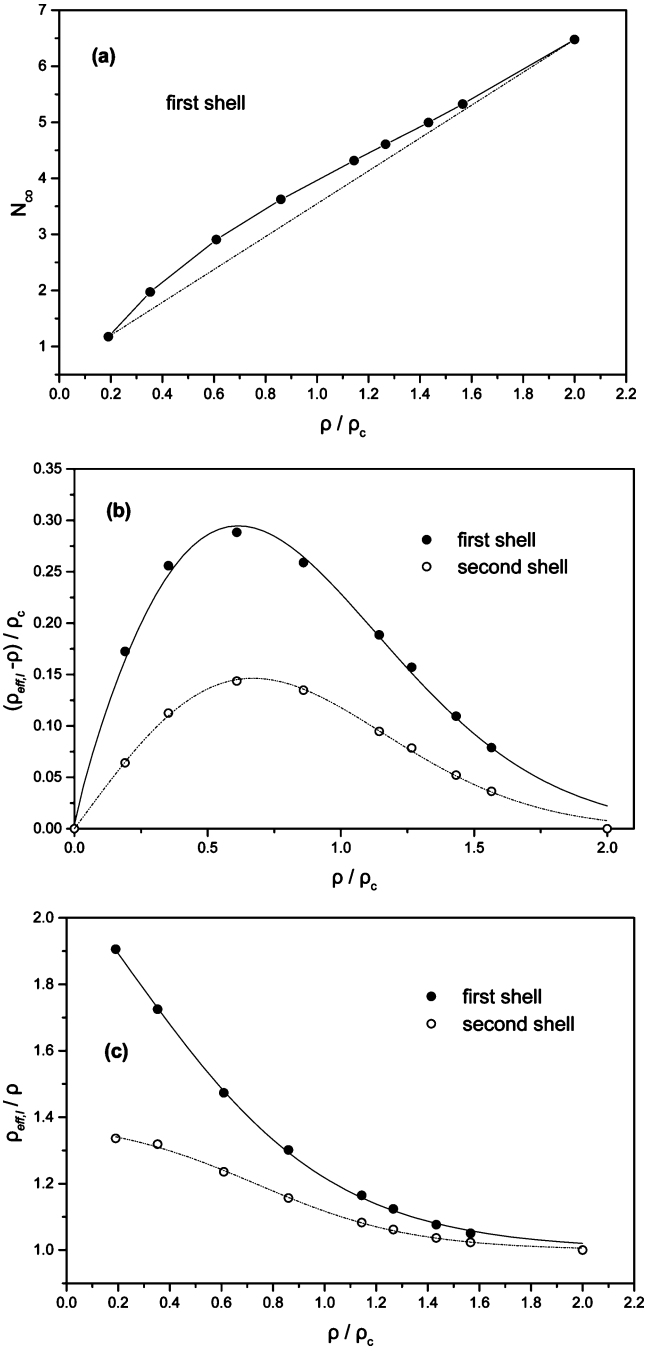

Figure 2. Calculated average coordination numbers, N_{co}, for the first coordination shell as a function of the reduced bulk density, ρ/ρ_c, are shown in (a). The calculated values of the local density augmentation, $\Delta\rho_{eff,l} = \rho_{eff,l} - \rho$, divided by the critical density, ρ_c, and the local density enhancement, $\rho_{eff,l}/\rho$, versus the reduced bulk density, ρ/ρ_c, are presented in (b), (c), respectively. The solid curve (first shell) and the dotted one (second shell) in (b), correspond to the fitted Weibull line shape function, while in (c) to the fitted sigmoidal Boltzmann function.

By inspecting the predicted N_{co} results from Figure 2a, we may observe that N_{co} is clearly nonlinear density dependent. It should be noted here that this nonlinearity of N_{co} against density indicates the presence of an average local density augmentation around the particles in the fluid. In view of the above, we have estimated the excess local density at different bulk densities of the fluid and the results are shown in Figures 2b and c. Concretely, Figure 2b shows the values of the "local density augmentation", $\Delta\rho_{eff,l} = \rho_{eff,l} - \rho$, divided by the critical density,ρ_c, in the region up to the first and second solvation shell of molecules in SCW as defined in Section 2. We mention that in a NVT-MD simulation, as in our case, it is appropriate to calculate the plots of $\Delta\rho_{eff,l}/\rho_c$ versus ρ/ρ_c by using the experimental critical density as reference and not the SPC/E estimated one. We recall here that the investigated densities are not predicted by the SPC/E potential model, since we have performed NVT and not NPT-MD simulations. Due to the box volume fluctuations, the NPT-MD method is not the appropriate one in calculating properties such as local density augmentation and not accurate in calculating the appropriate local density time correlation functions. Furthermore, due to the very small differences between the SPC/E estimated [40b] and experimental critical density the observed numerical differences in the local density augmentation are insignificant in both cases.

TABLE 2: Calculated Local Density Reorganization Times $\tau_{\Delta_{\rho l}}$ Corresponding to the First and Second Coordination Shell of SCW at $T/T_c = 1.03$

	SCW	
	$\tau_{\Delta_{\rho l}}$ (ps)	
state points	first shell	second shell
A	1.287	1.473
B	1.057	1.474
C	0.859	1.420
D	0.757	1.380
E	0.587	1.100
F	0.557	1.092
G	0.441	0.877
H	0.404	0.773
I	0.256	0.467

The corresponding results for the local density enhancement, $F_{enh} = (\rho_{eff,l}/\rho)$, are presented in Figure 2c. The smooth curves through the points in Figure 2b represent the best fits of the simulated data to the four-parameter a, b, c, and ρ_0 often proposed Weibull line shape function.[5]

$$\Delta\rho_{eff,l} = a\left(\frac{c-1}{c}\right)^{(1-c)/c}\left[\frac{\rho - \rho_0}{b} + \left(\frac{c-1}{c}\right)^{1/c}\right]^{c-1} \times \exp\left\{-\left[\frac{\rho-\rho_0}{b} + \left(\frac{c-1}{c}\right)^{1/c}\right]^{c} + \frac{c-1}{c}\right\} \quad (5)$$

The maximum value for $\Delta\rho_{eff,l}$ obtained from this fit represents the measure of the extent of the local density augmentation. In the case of the local density enhancement, F_{enh}, the curves through the points in Figure 2c represent the best fits of the simulated data to a model function. As mentioned in ref 5, in most cases an exponential function of the type, $F_{enh}(\rho) = 1 + a\exp(-b\rho)$, fits such data quite accurately. However, in the present study, the sets of F_{enh} data for SCW obtained up to the first and second shell cannot be reasonably fitted to the former function. We have found through trial fits of several model functions that a sigmoidal Boltzmann function, $F_{enh}(\rho) = 1 + \{(a-1)/[1 + \exp((\rho - \rho_0/b)]\}$, might be proposed as the most suitable one for the fit of these data.

As can be seen from Figure 2b, the effective local densities are augmented above ρ for densities smaller than 1.6 ρ_c. We mention also that the maximum value of $\Delta\rho_{eff,l}$ is found to be 0.292 ρ_c and 0.146 ρ_c for the first and second shell, respectively. Both $\Delta\rho_{eff,l}$ maximum values have been observed at 0.68 ρ_c. From Figure 2c, we can see that F_{enh} for the first solvation shell decreases from the gas-phase limit value $((\rho_{eff,l}/\rho))_0 = 2.10$ by increasing the bulk density, following a sigmoidal-Boltzman functional behavior. When the effective local density in the second solvation shell of molecules is considered, both the corresponding values of the maximum $\Delta\rho_{eff,l}$ and the gas-phase

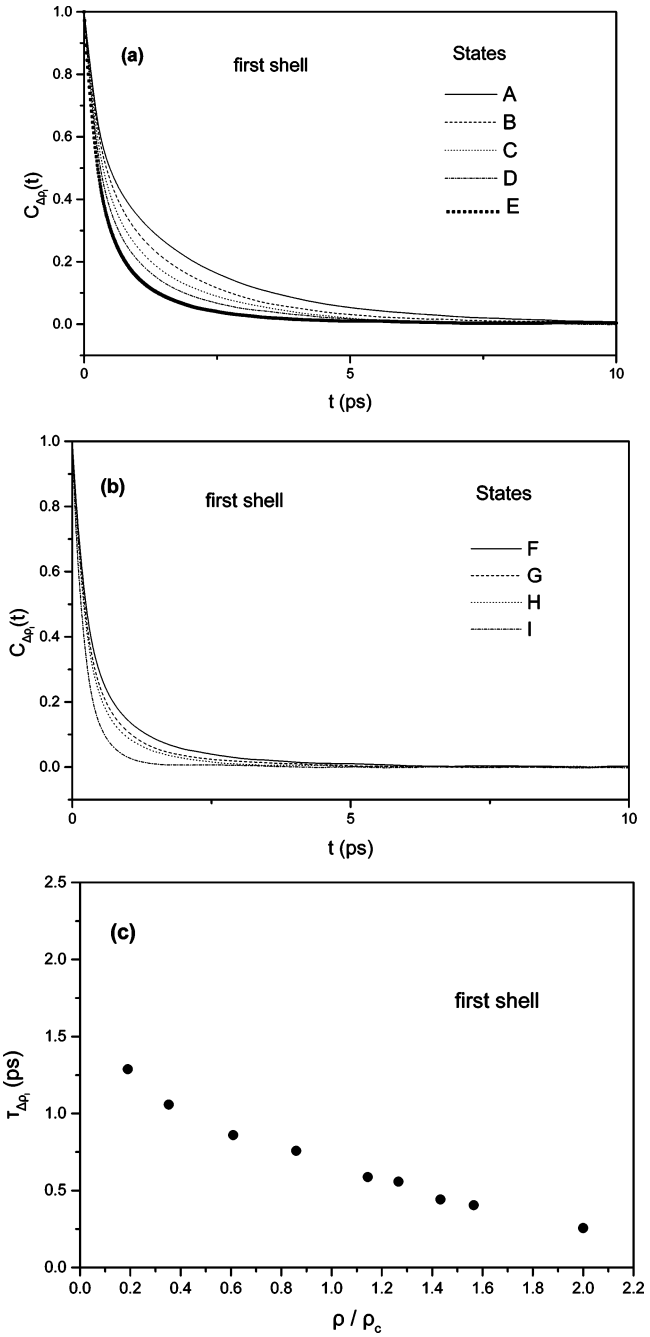

Figure 3. Calculated autocorrelation functions $C_{\Delta_{\rho l}}(t)$ for the local region corresponding to the first coordination shell at the thermodynamic state points A−E are presented in (a) and at F−I in (b). The bulk density dependence of the calculated local environment lifetimes $\tau_{\Delta_{\rho l}}$ for the first coordination shell is also depicted in (c).

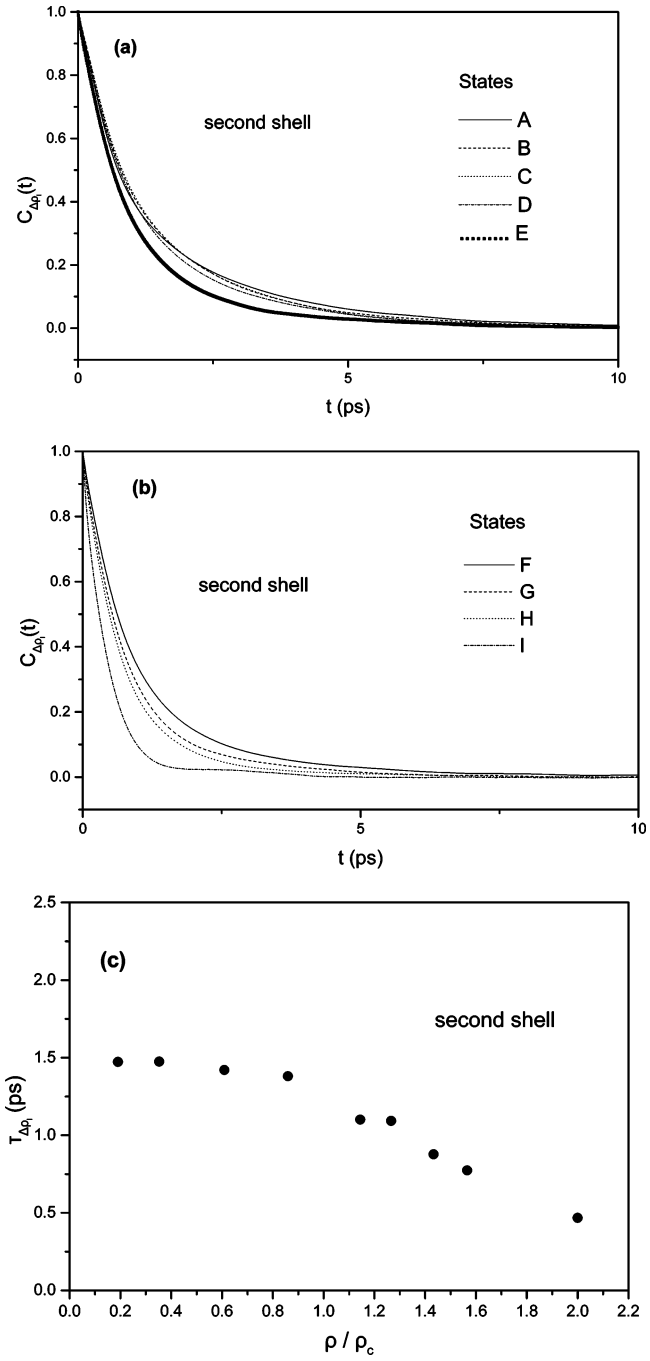

Figure 4. Calculated autocorrelation functions $C_{\Delta_{\rho l}}(t)$ for the local region corresponding to the second coordination shell at the thermodynamic state points A−E are presented in (a) and at F−I in (b). The bulk density dependence of the calculated local environment lifetimes $\tau_{\Delta_{\rho l}}$ for the second coordination shell is also depicted in (c).

limit value $((\rho_{\text{eff,l}}/\rho))_0 = 1.37$, decrease as expected. Note that the comparison of the present MD predictions for $\Delta\rho_{\text{eff,l}}$ or F_{enh} of pure SCW with results from suitable experiments might not be realizable due to the lack of such experimental information up to now.

We now focus on the average local density dynamics around the molecules in SCW. As we mentioned above, to shed some light on this specific problem, it is convenient to investigate the time dependent distribution of the local environment around the water molecules in terms of the tcf $C_{\Delta_{\rho l}}(t)$ defined by eq 3. We recall here that this function is particularly useful because its corresponding correlation time $\tau_{\Delta_{\rho l}}$ provides the local-density reorganization period. In Figures 3a, b and 4a, b we present the calculated tcfs $C_{\Delta_{\rho l}}(t)$ corresponding to the first and second coordination shell, respectively. The calculated local environment lifetimes $\tau_{\Delta_{\rho l}}$ against the bulk density are shown in Figures 3c and 4c and Table 2. By inspecting the results shown in these Figures, we may easily conclude that the lifetimes, $\tau_{\Delta_{\rho l}}$, depend on the size of the local region taken into account in our calculations. In other words, by extending the radius defining the local region up to the distance of the second coordination shell, we may observe a substantial increase of the local density lifetimes for all the investigated state points. Note that, the lifetimes $\tau_{\Delta_{\rho l}}$ obtained for the second shell at state points C−I are almost 2 times greater that those for the first one.

The aforementioned observations for pure SCW are found to be in agreement with previous preliminary simulation results reported on a two-dimensional pure monatomic LJ fluid model [see Figure 3 in ref 39b], according to which by increasing the size of the shell, the corresponding correlation time obtained also increases. To interpret their results, the authors in that study proposed the existence of two basic but different mechanisms for the creation of these local density fluctuations. The first one is assumed to take place in short length scales, which are in the range of the intermolecular interactions. This mechanism seems to have a very important contribution on the local structural effects observed at relatively low bulk densities. The second one results from indirect intermolecular interactions at more extended length scales, which are related to collective relaxation processes and they are maximized near the critical density. In our case, however, where we deal with a very strong hydrogen-bonded associated fluid such as SCW, even though one assumes that the two proposed mechanisms are valid here, they are not sufficiently capable in describing the more complicated reorganization processes occurring in associated fluids.

Concerning the bulk density dependence of the local density acfs, $C_{\Delta_{\rho l}}(t)$, of SCW from Figures 3a, b and 4a, b, we see that by increasing the bulk density (from state A to I), the time required for $C_{\Delta_{\rho l}}(t)$ to approach zero decreases significantly. For instance, from Figure 3a, b the$C_{\Delta_{\rho l}}(t)$ at state A decays to zero after approximately 10 ps, while at state I (highest density studied) after $\cong$ 2.5 ps. Furthermore, the local density lifetimes $\tau_{\Delta_{\rho l}}$ exhibit a decreasing behavior by increasing the bulk density. The decrease is especially larger in the range of densities higher than 1.2 ρ_c. From Figure 3c, we may observe a monotonic decrease in $\tau_{\Delta_{\rho l}}$ for the first shell, while from Figure 4c this correlation time for the second shell exhibits a plateau behavior in the low bulk density domain up to the critical one. At higher densities this correlation time shows a significant decrease. This behavior might be interpreted in terms of the bulk density effect upon the hydrogen bond structure and dynamics in SCW reported in previous CS studies.[46] It is pointed out that as the bulk density increases along an isotherm the lifetime of the hydrogen bonds decreases. Such a behavior might be explained in terms of the increase of the collisional events among the water molecules leading to a more frequent breaking of hydrogen bonds, and eventually to a faster local density reorganization process at the high bulk density region.

4. Conclusions

In this paper, the molecular dynamics simulation technique was used to investigate the features concerning the "Local Density Inhomogeneities and their Dynamics" in pure SCW. We have carried out atomistic simulations in the canonical statistical mechanical ensemble (NVT) along an isotherm, which is above the critical temperature ($T_r = T/T_c = 1.03$) and for densities below and above the critical one. Our calculations presented here are based on the capability of the extended simple point charge (SPC/E)[41] potential model of water to simulate the properties of the system not only at ambient but also at SC conditions.[40a]

The methodology employed to estimate the properties related to inhomogeneities in the fluid was based on the calculation of the excess local density (*augmentation)* relative to the bulk one, $\Delta\rho_{eff,l} = \rho_{eff,l} - \rho$, as well as the well-known *enhancement* factor $F_{enh} = (\rho_{eff,l}/\rho)$. The time evolution of the local density distribution around each molecule was studied in terms of the appropriate instantaneous local-density deviation relative to the mean local one acfs, $C_{\Delta_{\rho l}}(t)$.

The results obtained have shown that the effective average local densities in pure SCW are strongly augmented relative to the bulk ones. This behavior is observed in the bulk density region up to about 1.6 ρ_c. The estimated maximum value of $\Delta\rho_{eff,l}$ for the first shell (0.292 ρ_c) is about 2 times larger than that obtained for the second one (0.146 ρ_c), observed at the same bulk density of 0.68 ρ_c. We also note that the aforementioned $\Delta\rho_{eff,l}$ values for SCW are noticeably greater than the corresponding values obtained in previous simulations of other pure SC fluids.[12] Similar features are also obtained for the corresponding enhancement factors. This strong augmentation effect in SCW might be attributed to the compact hydrogen-bonding associative character of water in comparison with other non-associated fluids.

Concerning the local density dynamics in the fluid our results have indicated that the local density reorganization times $\tau_{\Delta_{\rho l}}$ exhibit a decreasing behavior by increasing the bulk density. This decrease is larger in the range of densities higher than 1.2 ρ_c. Additionally, for the first shell we observe a monotonic decrease with density in $\tau_{\Delta_{\rho l}}$, while for the second shell this reorganization time exhibits a plateau behavior in the low bulk density domain up to the critical one. This correlation time shows a significant decrease at higher densities, presumably due to the decrease of the hydrogen bond lifetimes.

Acknowledgment. We are grateful to the Research Oriented Computing Center John von Neumann-Institute (NIC-ZAM, Julich Germany) for the CPU time allocation on its supercomputing facilities. This work was supported by the National University of Athens-Greece grant no 70/4/6485.

References and Notes

(1) Johnston, K. P.; Kim, S.; Coumbes, J.; Penninger, J. M. L., Eds. *Supercritical Fluid Science and Technology*; American Chemical Society: Washington, DC, 1998; Chapter 5 and refs. therein.

(2) Kiran, E.; Debenedetti, P. G.; Peters, C. J., Eds. *Supercritical Fluids: Fundamentals and Applications*, NATO ASI Science Series E, Applied Sciences; Kluwer Academic Publishers: Dordrecht, The Netherlands, 2000; Vol. 366.

(3) Eckert, C. A.; Knutson, B. L.; Debenedetti, P. G. *Nature* **1996**, *383*, 313.

(4) (a) Tucker, S. C. *Chem. Rev.* **1999**, *99*, 391. (b) Kajimoto, O. *Chem. Rev.* **1999**, *99*, 355. (c) Fernandez-Prini, R.; Japas, M. L. *Chem. Soc. Rev.* **1994**, 155.

(5) (a) Song, W.; Biswas, R.; Maroncelli, M. *J. Phys. Chem. A* **2000**, *104*, 6924. (b) Lewis, J.; Biswas, R.; Robinson, A.; Maroncelli, M. *J. Phys. Chem. B* **2001**, *105*, 3306. (c) Rice, J. K.; Niemeyer, E. D.; Dunbar, R. A.; Bright, F. V. *J. Am. Chem. Soc.* **1995**, *117*, 5830. (d) Aizawa, T.; Kanakubo, M.; Ikushima, Y.; Smith Jr, R. L.; Saitoh, T.; Sugimoto, N. *Chem. Phys. Lett.* **2004**, *393*, 31.

(6) Echargui, M.; Marsault-Herail, F. *Mol. Phys.* **1987**, *60*, 605.

(7) Ben-Amotz, D.; LaPlant, F.; Shea, D.; Gardecki, J.; List, D. In *Supercritical Fluid Technology*; Bright F. V., McNally M. E., Eds.; ACS Symposium Series Vol. 488; American Chemical Society: Washington, DC, 1992; pp 18−30.

(8) Nakayama, H.; Saitow, K.; Nakashita, M.; Ishii, K.; Nishikawa, K. *Chem. Phys. Lett.* **2000**, *320*, 323.

(9) Cabaco, M. I.; Besnard, M.; Tassaing, T.; Danten, Y. *Pure Appl. Chem.* **2004**, *76*, 141.

(10) Maddox, M. W.; Goodyear, G.; Tucker, S. C. *J. Phys. Chem. B* **2000**, *104*, 6248.

(11) Egorov, A.; Yethiraj, A.; Skinner, J. L. *Chem. Phys. Lett.* **2000**, *317*, 558.

(12) Song, W.; Maroncelli, M. *Chem. Phys. Lett.* **2003**, *378*, 410.

(13) Egorov, S. A. *Chem. Phys. Lett.* **2002**, *354*, 140.

(14) Akiya, N.; Savage Ph. *Chem. Rev. (Washington, D. C.)* **2002**, *102*, 2725.

(15) (a) Hoffmann, M. M.; Conradi, M. S. *J. Am. Chem. Soc.* **1997**, *119*, 3811. (b) Bellissent-Funel, M. C.; Dore, J. C.; *Hydrogen Bond Networks*, NATO ASI Series, Series C: Mathematical and Physical Sciences 435; Kluwer Academic Publishers: Boston, MA, 1994.

(16) Postorino, P.; Tromp, R. H.; Ricci, M.-A.; Soper, A. K.; Nelson, G. W. *Nature (London)* **1993**, *366*, 668.

(17) Soper, A. K. *Chem. Phys.* **2000**, *258*, 121.

(18) (a) Gorbaty, Y. E.; Kalinichev, A. G. *J. Phys. Chem.* **1995**, *99*, 5336. (b) Morita, T.; Kusano, K.; Ochiai, H.; Saitow, K.; Nishikawa, K. *J. Chem. Phys.* **2000**, *112*, 4203.

(19) Wernet, Ph.; Testernale, D.; Hazemann, J.-L.; Argoud, R.; Glatzel, P.; Pettersson, L. G. M.; Nilsson, A.; Bergmann U. *J. Chem. Phys.* **2005**, *123*, art No 154503.

(20) Bellissent-Funel, M.-C.; Tassaing, T.; Zhao, H.; Beysens, D.; Guillot B.; Guissani, Y. *J. Chem. Phys.* **1997**, *107*, 2942.

(21) Matubayashi, N.; Wakai, C.; Nakahara, M. *J. Chem. Phys.* **1997**, *107*, 9133.

(22) Guissani, Y.; Guillot B. *J. Chem. Phys.* **1993**, *98*, 8221.

(23) Mountain, R. D. *J. Chem. Phys.* **1995**, *103*, 3084.

(24) Chialvo, A. A.; Cummings, P. T. *J. Phys. Chem.* **1996**, *100*, 1309.

(25) (a) Kalinichev, A. G.; Bass, J. D. *J. Phys. Chem.* **1997**, *101*, 9720. (b) Kalinichev, A. G.; Churakov, S. V. *Fluid Phase Equilib.* **2001**, *183*, 271. (c) Kalinichev, A. G.; Churakov, S. V. *Chem. Phys. Lett.* **1999**, *302*, 411.

(26) Mountain, R. D. *J. Chem. Phys.* **1998**, *110*, 2109.

(27) Jedlovszky, P.; Brodholt, J. B.; Bruni, F.; Ricci, M.-A.; Soper, A. K.; Vallauri, R. *J. Chem. Phys.* **1998**, *108*, 8528.

(28) Pártay, L.; Jedlovszky, P.*J. Chem. Phys.* **2005**, *123*, art. no. 024502.

(29) Fois, E. S.; Sprik, M.; Parinello, M. *Chem. Phys. Lett.* **1994**, *223*, 411.

(30) Boero, M.; Terakura, K.; Ikeshoji, T.; Liew, C. C.; Parinello, M. *J. Chem. Phys.* **2001**, *115*, 2219.

(31) Löfler, G.; Schreiber, H.; Steinhauser O. *Ber. Bunsen-Ges. Phys. Chem.* **1994**, *98*, 1575.

(32) Komatsu, T.; Yoshii, N.; Miura, S.; Okazaki, S. *Fluid Phase Equilib.* **2004**, *226*, 345.

(33) Chalaris, M.; Samios, J. *J. Phys. Chem. B* **1999**, *103*, 1161.

(34) Chatzis, G.; Samios, J. *Chem. Phys. Lett.* **2003**, *374*, 187.

(35) Chalaris, M.; Samios, J. *Pure Appl. Chem.* **2004**, *76*, 203.

(36) Dellis, D.; Chalaris, M.; Samios, J. *J. Phys. Chem. B* **2005**, *109*, 18575.

(37) Skarmoutsos, I.; Kampanakis, L. I.; Samios, J. *J. Mol. Liq.* **2005**, *117*, 33.

(38) Skarmoutsos, I.; Samios, J. *J. Mol. Liq.* **2006**, *125*, 181.

(39) (a) Tucker, S. C.; Maddox, M. W. *J. Phys. Chem. B* **1998**, *102*, *2437*. (b) Maddox, M. W.; Goodyear, G.; Tucker, S. C. *J. Phys. Chem. B* **2000**, *104*, 6266.

(40) (a) Guardia, E.; Marti, J. *Phys. Rev. E* **2004**, *69*, 011502. (b) Brovchenko, I.; Geiger, A.; Oleinikova, A. *J. Chem. Phys.* **2005**, *123*, 044515.

(41) Berendsen, H. J. C.; Grigera, J. R.; Straatsma, T. P. *J. Phys. Chem.* **1987**, *91*, 6269.

(42) Johansson, E.; Bolton, K.; Ahlström, P. *J. Chem. Phys.* **2005**, *123*, art. no. 024504.

(43) Berendsen, H. J. C.; Postma, J. P. M.; van Gunsteren, W. F.; DiNola, A.; Haak, J. R. *J. Chem. Phys.* **1984**, *81*, 3684.

(44) Ryckaert, J. P.; Ciccotti, G.; Berendsen, H. J. C. *J. Comput. Phys.* **1977**, *23*, 327.

(45) Paschek, D.; Geiger, A. *MOSCITO 4.1*; University of Dortmund: Dortmund, Germany, 2003.

(46) Mizan, T. I.; Savage, P. E.; Ziff, R. M. *J. Phys. Chem.* **1996**, *100*, 403.